
Research article

The Caputo fractional Windkessel model and cardiovascular circulatory system: Some approximate solutions in usual topological Banach spaces by using some techniques

Faten H. Damag^{1,2,*}

¹ Department of Mathematics, Faculty of Sciences, University of Ha'il, Ha'il 2440, Saudi Arabia

² Department of Mathematics, Faculty of Applied Sciences, Taiz University, Taiz 6803, Yemen

* **Correspondence:** Email: kilicman@uitm.edu.my.

Abstract: The Windkessel model is a lumped-parameter representation that simplifies the complex cardiovascular system into an equivalent hydraulic circuit comprising resistive and compliant components. It plays a crucial role in understanding the dynamics of blood flow and pressure within the circulatory system, especially in the arterial network. In this study, we employ the Caputo fractional operator to obtain approximate solutions for the Windkessel model within the framework of usual topological Banach spaces. An efficient hybrid analytical technique, termed the Aboodh residual power series method (ARPSM), has been developed by integrating the Aboodh transform with the residual power series method. This approach is used to investigate and derive approximate solutions of the modified Caputo fractional Windkessel model. The accuracy, reliability, and applicability of the proposed ARPSM are demonstrated through numerical and graphical analyses, confirming its effectiveness in solving fractional differential equations of this type.

Keywords: Residual power series; Aboodh transform; Caputo derivative operator

Mathematics Subject Classification: Primary 44A10, 33B15, 34A34, 35A20

1. Introduction

The theory of differential equations is considered one of the most important subjects in a wide field of sciences, where its applications extend to several branches such as physics, mathematics, medicine, wave theory, and fluid mechanics, among others. In recent years, several studies have appeared on the subject of fractional calculus, which is regarded as a practical tool and a dynamic field of mathematics for generalizing integer-order equations to their fractional orders. This generalization enables the solution of a wide range of equations and leads to the formulation of fractional differential equations, thereby introducing a new class of mathematical frameworks for analyzing complex

dynamical systems; for more details. For example, a fractional comparison of the Camassa–Holm and Degasperis–Procesi equations was given in [1], approximate controllability for mixed-type fractional systems was studied in [2], the existence of mild solutions for fractional evolution equations with delay was shown in [3], and Laplace residual power series method for fractional Kawahara equations was proposed in [4]. These extensive studies have shown that fractional differential equations provide a powerful framework with numerous applications in various fields such as electrical networks, groundwater modeling, physics, fluid mechanics, engineering, medicine, and many other areas of science. Several notions of fractional derivatives have been developed, among which the Riemann–Liouville fractional differential operator is the most classical and well-known. Using the concept of the Riemann–Liouville operator, many researchers have introduced and investigated other fractional differential operators such as the Hilfer fractional derivative, the ϕ derivative, and the Hilfer–Katugampola fractional derivative. Regarding integral operators, the Riemann–Liouville fractional integral operator is also considered the oldest and most famous among the classes of fractional integral operators. Based on its concept, other integral operators such as the Hadamard fractional integral and the Katugampola fractional integral were later proposed. For more details on fractional integral and differential operators, the fuzzy fractional PDEs were studied in [5]. Complex solutions for Boussinesq-type equations were found in [6]. Mild solutions for fractional reaction-diffusion delays were proved in [7]. Fractional Kawahara equations were compared analytically and numerically in [8]. Existence and stability for mixed Hilfer equations were shown in [9]. A fractional Newton method was developed in [10]. ϕ -Hilfer fractional Cauchy problems were analyzed in [11]. Hyperbolic wave solutions for the Wu–Zhang system were given in [12]. One of the important applications of both ordinary and fractional differential equations is found in the study of the Windkessel model, which represents one of the most significant models describing the dynamic behavior of arteries in the cardiovascular circulatory system. This model helps in understanding the dynamics of blood circulation and the effects of various physiological parameters on blood pressure and flow [13]. The Windkessel model conceptualizes the arterial system as a compliant reservoir that absorbs the pulsatile output of the heart and maintains a steady flow of blood during diastole. The relationship between blood flow and pressure in the cardiovascular circulatory system is expressed by the following differential equation [14]:

$$\mu \frac{d\zeta(\tau)}{d\tau} + \frac{1}{\eta} \zeta(\tau) = Q(\tau) \quad 0 < \delta \leq 1 \quad (1.1)$$

where $\zeta(\tau)$ is the pressure of arteries at time τ , $Q(\tau)$ is the blood flow rate at τ , η is the total vascular resistance, and the μ is the total compliance of the arterial system. For providing analysis and approximation solutions of Windkessel model, there are several studies for example, Gnudi, [15], derived the time-domain analytical solutions to two-, three-, and four-element Windkessel models and then he obtained a closed-form expressions for arterial system. Gil et al., [16], presented results and analysis concerning a two-element Windkessel model to account for the compliance and vascular resistance of the arterial system. Fernandes et al., [17], pioneered a novel approach that combines physiologically accurate models with a five-element Windkessel model to enhance the accuracy of hemodynamics and the fractional flow reserve parameter. Westerhof et al., [18], introduced characteristic impedance as a third element of the Windkessel model to estimate total arterial compliance based on blood flow and pressure. Choudhury et al., [19], used the two-element Windkessel model to estimate total peripheral resistance and arterial compliance in a person utilizing some features.

Kind et al., [20], employed a non-iterative identification algorithm that utilized physical foreknowledge to estimate parameters in both the three-element and four-element Windkessel models. Several studies introduced approximate solutions and analysis of Windkessel models by using fractional operator, for example, Gamilov and Ruslan, [21], proposed combining a one-dimensional model of coronary blood flow with fractional-order Windkessel boundary conditions. Bahloul and Taous [22], proved that the fractional-order Windkessel model better fits the moduli of aortic input impedance and accurately approximates the phase angle. Traver et al., [23], demonstrated the effectiveness of fractional-order behavior in the classic Windkessel model. Resmi and Selvanesani, [24], introduced fractionality in the existing 2-element, 3-element and 4-element Windkessel models.

Recall [25] that the usual topological Banach space is a collection of a Banach space \mathcal{B} over a field \mathbb{F} and a norm $\|\cdot\|$ on \mathcal{B} with metrizable topology induced by $\|\cdot\|$. Let $\zeta(\tau) : (0, \infty) \rightarrow \mathcal{B}$ be any function on $\mathbb{J} := (0, \infty)$. The motivation of this study arises from the need to extend the classical Windkessel model into a more general fractional framework that captures the inherent memory and hereditary effects of the cardiovascular system. The traditional integer-order models are limited in describing the viscoelastic and non-local properties of blood flow and arterial walls, whereas fractional calculus provides a more flexible and accurate representation of such physiological phenomena. In particular, incorporating the Caputo fractional derivative allows the model to handle realistic initial conditions and describe the dynamic behavior of arterial pressure and blood flow with higher precision. To achieve this goal, we employ the ARPSM, a hybrid analytical approach that combines the Aboodh transform with the residual power series technique. This method offers several advantages, including simplicity, convergence reliability, and computational efficiency, making it suitable for solving complex fractional differential equations. Therefore, the principal aim of this work is to develop and apply the ARPSM to obtain approximate analytical solutions of the Caputo fractional Windkessel model formulated within the usual topological Banach space $\mathcal{B} = \mathbb{R}$. Through this approach, we aim to provide a deeper mathematical and physiological understanding of the influence of fractional parameters on arterial blood pressure and flow dynamics. In this work, we use the technique ARPSM to find some approximate solutions of the following fractional differential equation in the usual topological Banach space $\mathcal{B} = \mathbb{R}$

$$\mu {}^c\mathcal{D}^\delta \zeta(\tau) + \frac{1}{\eta} \zeta(\tau) = Q(\tau) \quad (1.2)$$

where ${}^c\mathcal{D}^\delta$ is the Caputo fractional derivative operator of order δ , $\zeta(\tau)$ in the framework of the usual topological Banach space $\mathcal{B} = \mathbb{R}$, where ${}^c\mathcal{D}^\delta$ denotes the Caputo fractional derivative of order δ . The objective is to obtain approximate analytical solutions that demonstrate the influence of fractional parameters on blood flow and pressure, thereby providing a deeper physiological interpretation of circulatory system dynamics. Section 2 introduces basic concepts and essential facts about Caputo fractional derivative operators and the Aboodh transform. Several fundamental properties of these operators are established in the framework of usual topological Banach spaces. Section 3 presents the main steps and analytical formulation of the ARPSM technique. In Section 4, approximate solutions of the fractional differential equation (1.2), representing the Caputo fractional Windkessel model, are derived. Section 5 provides numerical and graphical demonstrations of the obtained results to illustrate the efficiency, reliability, and capability of the ARPSM in finding accurate approximate solutions. Finally, Section 6 discusses the findings and presents concluding remarks.

2. On Caputo operator and Aboodh transform

Consider ω to be any piecewise continuous function on \mathbb{J} . The R-LF derivative, [26], for $\omega(\sigma)$ of order $\delta > 0$ is given by

$$\mathcal{D}^\delta \omega(\sigma) = \mathcal{D}^m I^\delta \omega(\sigma) \quad m-1 < \delta < m \quad (2.1)$$

where $m \in \mathbb{N}$ and I^δ is the R-LF integral, [26], for $\omega(\sigma)$ of order δ is given by

$$I^\delta \omega(\sigma) = \begin{cases} \frac{1}{\Gamma(\delta)} \int_0^\sigma (\sigma - \tau)^{\delta-1} \omega(\tau) d\tau, & \delta > 0 \\ \omega(\sigma), & \delta = 0. \end{cases} \quad (2.2)$$

The CFD operator, [27], for $\omega(\sigma)$ of order δ is given by

$${}^c \mathcal{D}^\delta \omega(\sigma) = \begin{cases} I^{m-\delta} \left[\frac{d^m \omega(\sigma)}{d\sigma^m} \right], & m-1 < \delta < m \\ \frac{d^\delta \omega(\sigma)}{d\sigma^\delta}, & \delta \in \mathbb{N}, \end{cases} \quad (2.3)$$

Recall [27] that for $\sigma \geq 0$ and for $m-1 < \delta < m$ we have ${}^c \mathcal{D}^\delta I^\delta \omega(\sigma) = \omega(\sigma)$ and ${}^c \mathcal{D}^\delta \sigma^\gamma = \frac{\Gamma(\delta+1)}{\Gamma(\gamma-\delta+1)} \sigma^{\gamma-\delta}$.

Let $\omega(\sigma)$ be any continuous function on \mathbb{J} and with exponential order α . The Aboodh transform A_θ , [28], of $\omega(\sigma)$ is

$$\omega^A(\theta) := A_\theta \omega(\sigma) = \frac{1}{\theta} \int_0^\infty e^{-\theta\sigma} \omega(\sigma) d\sigma \quad \alpha_1 \leq \theta \leq \alpha_2. \quad (2.4)$$

The inverse Aboodh transform A_θ^{-1} of $\omega^A(\theta)$ is given by

$$\omega(\sigma) := A_\theta^{-1} \omega^A(\theta) = \frac{1}{2\pi i} \int_{d-i\infty}^{d+i\infty} \theta e^{\sigma\theta} \omega^A(\theta) d\theta. \quad (2.5)$$

In the following lemmas and Theorems, consider \mathcal{B} to be a usual topological Banach space $\mathcal{B} = \mathbb{R}$ over a field $\mathbb{F} = \mathbb{R}$. The proof of the following lemma is straightforward in usual topological Banach space, [29].

Lemma 2.1. Let $\omega, \varepsilon : \mathbb{J} \rightarrow \mathcal{B}$ be any function on \mathbb{J} . Then

1. $A_\theta[c_1 \omega(\sigma) + c_2 \varepsilon(\sigma)] = c_1 A_\theta \omega(\sigma) + c_2 A_\theta \varepsilon(\sigma)$, where c_1 and c_2 are constants;
2. $A_\theta^{-1}[c_1 A_\theta \omega(\sigma) + c_2 A_\theta \varepsilon(\sigma)] = c_1 \omega(\sigma) + c_2 \varepsilon(\sigma)$, where c_1 and c_2 are constants;
3. $A_\theta I^\delta \omega(\sigma) = \theta^{-\delta} \omega^A(\theta)$;
4. $A_\theta [{}^c \mathcal{D}^\delta \omega(\sigma)] = \theta^\delta \omega^A(\theta) - \sum_{j=0}^{n-1} \theta^{\delta-j-2} \frac{d^j}{d\sigma^j} \omega(\sigma) \Big|_{\sigma=0} \quad (n-1 < \delta < n)$.

Recall [30] that the power series form reads

$$\sum_{j=0}^{\infty} \omega_j(\sigma) (\mathcal{Y} - \mathcal{Y}_0)^{jn} = \omega_0(\sigma) (\mathcal{Y} - \mathcal{Y}_0)^0 + \omega_1(\sigma) (\mathcal{Y} - \mathcal{Y}_0)^n + \omega_2(\sigma) (\mathcal{Y} - \mathcal{Y}_0)^{2n} + \cdots \quad (2.6)$$

where $\sigma = (\sigma_1, \sigma_2, \dots, \sigma_n) \in \mathbb{R}^n, n \in \mathbb{N}$. The series about \mathcal{Y}_0 with \mathcal{Y} as a variable and the series coefficients $\omega_j(\sigma)$ is called a multiple fractional power series (MFPS).

Lemma 2.2. Let $\omega : \mathbb{J} \rightarrow \mathcal{B}$ be a continuous function on \mathbb{J} . Then

$$A_\theta \left[{}^c\mathcal{D}^{k\delta} \omega(\sigma) \right] = \theta^{k\delta} \omega^A(\theta) - \sum_{j=0}^{k-1} \theta^{(k-j)\delta-2} {}^c\mathcal{D}^{j\delta} \omega(\sigma) \Big|_{\sigma=0} \quad (0 < \delta \leq 1). \quad (2.7)$$

Proof. We will prove Eq (2.7) by mathematical induction. At $k = 1$, since $0 < \delta \leq 1$ in Eq (2.7), that is, $n = 0$ in the part (4) of Lemma above. Hence

$$A_\theta \left[{}^c\mathcal{D}^\delta \omega(\sigma) \right] = \theta^\delta \omega^A(\theta) - \theta^{\delta-2} \omega(0). \quad (2.8)$$

That is, Eq (2.7) holds at $k = 1$. At $k = 2$, let $\varepsilon(\sigma) = {}^c\mathcal{D}^\delta \omega(\sigma)$. Then by using Eq (2.8) above we get that

$$\begin{aligned} A_\theta \left[{}^c\mathcal{D}^\delta \varepsilon(\sigma) \right] &= \theta^\delta \varepsilon^A(\theta) - \theta^{\delta-2} \varepsilon(0) \\ &= \theta^\delta A_\theta {}^c\mathcal{D}^\delta \omega(\sigma) - \theta^{\delta-2} {}^c\mathcal{D}^\delta \omega(\sigma) \Big|_{\sigma=0} \\ &= \theta^\delta \left[\theta^\delta \omega^A(\theta) - \theta^{\delta-2} \omega(0) \right] - \theta^{\delta-2} {}^c\mathcal{D}^\delta \omega(\sigma) \Big|_{\sigma=0} \\ &= \theta^{2\delta} \omega^A(\theta) - \theta^{2\delta-2} \omega(0) - \theta^{\delta-2} {}^c\mathcal{D}^\delta \omega(\sigma) \Big|_{\sigma=0}. \end{aligned} \quad (2.9)$$

That is, Eq (2.7) holds at $k = 2$. Suppose that Eq (2.7) holds at $k = m$, that is,

$$A_\theta \left[{}^c\mathcal{D}^{m\delta} \omega(\sigma) \right] = \theta^{m\delta} \omega^A(\theta) - \sum_{j=0}^{m-1} \theta^{(m-j)\delta-2} {}^c\mathcal{D}^{j\delta} \omega(\sigma) \Big|_{\sigma=0}. \quad (2.10)$$

We will prove that Eq (2.7) holds at $k = m + 1$. Let $\varepsilon(\sigma) = {}^c\mathcal{D}^{m\delta} \omega(\sigma)$. Then by using Eq (2.8) and Eq (2.10) we get that

$$\begin{aligned} A_\theta \left[{}^c\mathcal{D}^{k\delta} \varepsilon(\sigma) \right] &= \theta^\delta A_\theta {}^c\mathcal{D}^{m\delta} \omega(\sigma) - \theta^{\delta-2} {}^c\mathcal{D}^{m\delta} \omega(\sigma) \Big|_{\sigma=0} \\ &= \theta^\delta \left[\theta^{m\delta} \omega^A(\theta) - \sum_{j=0}^{m-1} \theta^{(m-j)\delta-2} {}^c\mathcal{D}^{j\delta} \omega(\sigma) \Big|_{\sigma=0} \right] \\ &\quad - \theta^{\delta-2} {}^c\mathcal{D}^{m\delta} \omega(\sigma) \Big|_{\sigma=0} \\ &= \theta^{(m+1)\delta} \omega^A(\theta) - \sum_{j=0}^{m-1} \theta^{(m+1-j)\delta-2} {}^c\mathcal{D}^{j\delta} \omega(\sigma) \Big|_{\sigma=0} \\ &\quad - \theta^{\delta-2} {}^c\mathcal{D}^\delta \omega(\sigma) \Big|_{\sigma=0} \\ &= \theta^{(m+1)\delta} \omega^A(\theta) - \sum_{j=0}^m \theta^{(m+1-j)\delta-2} {}^c\mathcal{D}^{j\delta} \omega(\sigma) \Big|_{\sigma=0} \\ &= \theta^{k\delta} \omega^A(\theta) - \sum_{j=0}^{k-1} \theta^{(k-j)\delta-2} {}^c\mathcal{D}^{j\delta} \omega(\sigma) \Big|_{\sigma=0} \end{aligned} \quad (2.11)$$

Hence Eq (2.7) holds for all $k \in \mathbb{N}$. □

Lemma 2.3. Let $\omega : (0, \infty)^n \rightarrow \mathcal{B}$ be an exponential order function. Then the MFPS notation for Aboodh transform will be

$$\omega^A(\theta) = \sum_{j=0}^{\infty} \frac{f_j(\sigma)}{\theta^{jn+2}} \quad \theta > 0, \quad (2.12)$$

where $\sigma = (\sigma_1, \sigma_2, \dots, \sigma_n) \in (0, \infty)^n, n \in \mathbb{N}$.

Proof. Use Taylor series fractional order expression to get

$$\omega(\sigma) = f_0(\sigma) + f_1(\sigma) \frac{\mathcal{Y}^n}{\Gamma(n+1)} + f_2(\sigma) \frac{\mathcal{Y}^{2n}}{\Gamma(2n+1)} + \dots \quad (2.13)$$

Take Aboodh transform for Eq (2.12) to get

$$\begin{aligned} A_\theta \omega(\sigma) &= A_\theta f_0(\sigma) + f_1(\sigma) \frac{A_\theta \mathcal{Y}^n}{\Gamma(n+1)} + f_2(\sigma) \frac{A_\theta \mathcal{Y}^{2n}}{\Gamma(2n+1)} + \dots \\ &= \frac{f_0(\sigma)}{\theta^2} + f_1(\sigma) \frac{\Gamma(n+1)}{\theta^{n+2} \Gamma(n+1)} + f_2(\sigma) \frac{\Gamma(2n+1)}{\theta^{2n+2} \Gamma(2n+1)} + \dots \\ &= \sum_{j=0}^{\infty} \frac{f_j(\sigma)}{\theta^{jn+2}} \end{aligned} \quad (2.14)$$

□

Lemma 2.4. Let $\omega : (0, \infty)^n \rightarrow \mathcal{B}$ be an exponential order continuous function. Then $\lim_{\theta \rightarrow \infty} \theta^2 \omega^A(\theta) = \omega(0)$ for all $\sigma \in (0, \infty)^n$.

Proof. Take $\omega(0) = f_0(\sigma)$ to get the desired. □

Theorem 2.5. Let $\omega : (0, \infty)^n \rightarrow \mathcal{B}$ be an exponential order continuous function. Then

$$\omega^A(\theta) = \sum_{j=0}^{\infty} \frac{f_j(\sigma)}{\theta^{jn+2}} \quad (0 < \delta \leq 1) \quad (2.15)$$

for all $\sigma \in (0, \infty)^n$ and $\theta > 0$, where $f_j(\sigma) = \frac{d^{jn}}{d\sigma^{jn}} \omega(\sigma) \Big|_{\sigma=0}$.

Proof. The new form of Taylor's series will be as follows:

$$f_1(\sigma) = \theta^{n+2} \omega^A(\theta) - \theta^n f_0(\sigma) - \frac{1}{\theta^n} f_2(\sigma) - \frac{1}{\theta^{2n}} f_3(\sigma) - \dots \quad (2.16)$$

Take the limit of Eq (2.16) when $\theta \rightarrow \infty$ to get

$$f_1(\sigma) = \lim_{\theta \rightarrow \infty} \left[\theta^{n+2} \omega^A(\theta) - \theta^n f_0(\sigma) \right]. \quad (2.17)$$

By Lemma 2.2

$$f_1(\sigma) = \lim_{\theta \rightarrow \infty} \theta^2 A_\theta \left[\frac{d^n}{d\sigma^n} \omega(\sigma) \right]. \quad (2.18)$$

By Lemma 2.4 we get $f_1(\sigma) = \frac{d^n}{d\sigma^n} \omega(\sigma) \Big|_{\sigma=0}$. Similar, the new form of Taylor's series of f_2 will be as follows:

$$f_2(\sigma) = \theta^{2n+2} \omega^A(\theta) - \theta^{2n} f_0(\sigma) - \theta^n f_1(\sigma) - \frac{1}{\theta^n} f_3(\sigma) - \frac{1}{\theta^{2n}} f_4(\sigma) - \dots \quad (2.19)$$

Take the limit of Eq (2.19) when $\theta \rightarrow \infty$ to get

$$f_2(\sigma) = \lim_{\theta \rightarrow \infty} \left[\theta^{2n+2} \omega^A(\theta) - \theta^{2n} f_0(\sigma) - \theta^n f_1(\sigma) \right]. \quad (2.20)$$

By Lemmas 2.2 and 2.4 we get $f_2(\sigma) = \frac{d^{2n}}{d\sigma^{2n}} \omega(\sigma) \Big|_{\sigma=0}$. By the continuity, we indicate that $f_j(\sigma) = \frac{d^{jn}}{d\sigma^{jn}} \omega(\sigma) \Big|_{\sigma=0}$. \square

In theorem above we get that

$$A_\theta \left[{}^c \mathcal{D}^\delta \omega(\sigma) \right] = \sum_{j=0}^{\infty} \frac{1}{\theta^{j\delta+2}} {}^c \mathcal{D}^{j\delta} \omega(\sigma) \Big|_{\sigma=0} \quad (0 < \delta \leq 1)$$

for all $\sigma \in \mathbb{R}^n$, $\theta > 0$ and the inverse Aboodh transform is given by:

$$\omega(\sigma) = \sum_{j=0}^{\infty} \frac{{}^c \mathcal{D}^{j\delta} \omega(\sigma) \Big|_{\sigma=0}}{\Gamma(j\delta + 2)} \mathcal{Y}^{j\delta} \quad (0 < \delta \leq 1)$$

for all $\sigma \in \mathbb{R}^n$ and $\mathcal{Y} > 0$.

Theorem 2.6. Let $\omega : \mathbb{R}^n \times (0, \infty) \rightarrow \mathcal{B}$ be a exponential order continuous function. If $\left\| \theta^r A_\theta \left[{}^c \mathcal{D}^{(n+1)\delta} \omega(\sigma) \right] \right\| \leq M$ for all $0 < \theta \leq q$ and $0 < \delta \leq 1$ then the residual $\mathcal{R}es_n(\theta)$ of MFPS satisfies $\|\mathcal{R}es_n(\theta)\| \leq \frac{M}{\theta^{(n+1)\delta}}$.

Proof. Take the new form of Taylor's series as

$$\mathcal{R}es_n(\theta) = \omega^A(\theta) + \sum_{j=0}^n \frac{f_j(\sigma)}{\theta^{j\delta+2}}. \quad (2.21)$$

By Theorem 2.5 we get

$$\mathcal{R}es_n(\theta) = \omega^A(\theta) + \sum_{j=0}^n \frac{{}^c \mathcal{D}^{j\delta} \omega(0)}{\theta^{j\delta+2}}. \quad (2.22)$$

Multiply Eq (2.22) by $\theta^{(n+1)\delta}$ to get

$$\theta^{(n+1)\delta} \mathcal{R}es_n(\theta) = \theta^{(n+1)\delta} \omega^A(\theta) + \sum_{j=0}^n \theta^{(n+1-j)\delta-2c} {}^c \mathcal{D}^{j\delta} \omega(0). \quad (2.23)$$

By Lemma 2.2 we get

$$\theta^{(n+1)\delta} \mathcal{R}es_n(\theta) = A_\theta \left[{}^c \mathcal{D}^{(n+1)\delta} \omega(\sigma) \right]. \quad (2.24)$$

Hence

$$\left\| \theta^{(n+1)\delta} \mathcal{R}es_n(\theta) \right\| = \left\| A_\theta \left[{}^c \mathcal{D}^{(n+1)\delta} \omega(\sigma) \right] \right\|.$$

That is, $\|\mathcal{R}es_n(\theta)\| \leq \frac{M}{\theta^{(n+1)\delta}}$. \square

3. The methodology of ARPSM

The ARPSM is one of methods that introduced and used by mathematical researchers to get the approximate solutions of fractional differential equations. For example, Liaqat et al., [29] developed a novel analytic technique ARPSM to obtain the exact and approximate solutions of the Caputo time-fractional partial differential equations with variable coefficients. Liaqat et al., [29] used ARPSM to get some results of the Black-Scholes differential equations Noor et al., [28] used ARPSM to get some approximate solutions for some partial differential equations with one-dimensional nonlinear shock waves. Edalatpanah and Abdolmaleki, [31] used ARPSM to provide some results of the N-Wh-S equation. They got simplicity of this method. Yasmin and Almuqrin, [30] used ARPSM to get some results.

Here we present the ARPSM steps in solving differential equations. Consider the CFD equation:

$${}^c\mathcal{D}^\delta \omega(\sigma) = \mathcal{N}(\omega(\sigma)) + \mathcal{M}(\omega(\sigma)) \quad \delta \in (0, 1] \quad (3.1)$$

where $\omega : \mathbb{J} \rightarrow \mathcal{B}$ is a piecewise continuous function, \mathcal{N} denotes nonlinear part depending on the function $\omega(\sigma)$ of variable σ while \mathcal{M} denotes the function. The initial conditions play a role in getting the overall behavior of terms \mathcal{M} and \mathcal{N}

$$\omega(\sigma_0) = r_0. \quad (3.2)$$

Use the Aboodh transform A_θ of Eq (3.1)

$$A_\theta \left[{}^c\mathcal{D}^\delta [\omega(\sigma)] \right] = A_\theta [\mathcal{N}(\omega(\sigma))] + A_\theta [\mathcal{M}(\omega(\sigma))]. \quad (3.3)$$

By Lemma 2.1, the Aboodh transform A_θ for the left side of Eq (3.3) becomes

$$A_\theta \left[{}^c\mathcal{D}^\delta \omega(\sigma) \right] = \theta^\delta \omega^A(\theta) - \theta^{\delta-2} r_0. \quad (3.4)$$

Then from Eqs (3.3) and (3.4) we obtain that

$$\omega^A(\theta) = \frac{1}{\theta^2} r_0 + \frac{1}{\theta^\delta} A_\theta \left[\mathcal{N}(A_\theta^{-1}(\omega^A(\theta))) \right] + \frac{1}{\theta^\delta} A_\theta \left[\mathcal{M}(A_\theta^{-1}(\omega^A(\theta))) \right]. \quad (3.5)$$

The power series solution $\omega^A(\theta)$ for Eq (3.3) is given by

$$\omega^A(\theta) = \frac{1}{\theta^2} r_0 + \sum_{j=1}^{\infty} \frac{r_j}{\theta^{j\delta+2}}. \quad (3.6)$$

By the initial condition in Eq (3.1) and Lemma 2.1, we give the sequence $\langle \omega_n^A \rangle_{n \in \mathbb{N} \cup \{0\}}$ of the above series in Eq (3.6) as

$$\omega_n^A(\theta) = \frac{1}{\theta^2} r_0 + \sum_{j=1}^n \frac{r_j}{\theta^{j\delta+2}}. \quad (3.7)$$

Now construct the residual function of Aboodh transform, $A_\theta \text{Res } \omega$ for Eq (3.5) as follow:

$$A_\theta \text{Res } \omega = \omega^A(\theta) - \frac{1}{\theta^2} r_0 - \frac{1}{\theta^\delta} A_\theta \left[\mathcal{N}(A_\theta^{-1}(\omega^A(\theta))) \right] - \frac{1}{\theta^\delta} A_\theta \left[\mathcal{M}(A_\theta^{-1}(\omega^A(\theta))) \right] \quad (3.8)$$

and the n -th Aboodh residual function $A_\theta \mathcal{R}es_n \omega$ is

$$A_\theta \mathcal{R}es_n \omega = \omega_n^A(\theta) - \frac{1}{\theta^2} r_0 - \frac{1}{\theta^\delta} A_\theta \left[\mathcal{N}(A_\theta^{-1}(\omega_n^A(\theta))) \right] - \frac{1}{\theta^\delta} A_\theta \left[\mathcal{M}(A_\theta^{-1}(\omega_n^A(\theta))) \right]. \quad (3.9)$$

Note that $A_\theta \mathcal{R}es \omega = 0$ and

$$\lim_{n \rightarrow \infty} A_\theta \mathcal{R}es_n \omega = A_\theta \mathcal{R}es \omega$$

for all $\theta > 0$. Note that if $\lim_{\theta \rightarrow \infty} \theta^2 A_\theta \mathcal{R}es \omega = 0$ then $\lim_{\theta \rightarrow \infty} \theta^2 A_\theta \mathcal{R}es_n \omega = 0$. In general, if $\lim_{\theta \rightarrow \infty} \theta^{n\delta+2} A_\theta \mathcal{R}es \omega = 0$ then $\lim_{\theta \rightarrow \infty} \theta^{n\delta+2} A_\theta \mathcal{R}es_n \omega = 0$ and $0 < \delta \leq 1$. To obtain the coefficients r_n , we solve the following

$$\lim_{\theta \rightarrow \infty} \theta^{n\delta+2} A_\theta \mathcal{R}es_n \omega = 0. \quad (3.10)$$

4. Approximate solutions

In this section, we will use the technique of ARPSM above to get some approximate solutions of the fractional differential equation (1.2) in the usual topological Banach space $\mathcal{B} = \mathbb{R}$. It is clear that the equation represents the two-element Windkessel model which describes the relation between the arterial pressure at and $Q(\tau)$ is the blood flow rate at time τ as shown graphically in Figure 1c. As we know, the cardiac cycle is a closed-loop, pulsatile system in which the heart pumps blood throughout the systemic circulation, resembling a pulse wave, see Figure 1a, [32]. Windkessel models are commonly used to present the load on the heart when pumping blood in arterial systems, as well as the relation between blood pressure and flow with the pulmonary artery as shown graphically in Figure 1b and c. Figure 1 illustrates the schematic representation of the *two-element Windkessel model* in the human circulatory system. Panel (a) shows the cardiac cycle, emphasizing the pulsatile nature of blood flow generated by the heart. Panel (b) depicts the pulmonary and systemic arterial connections, highlighting the continuous circulation through the heart and major vessels. Panel (c) presents the equivalent hydraulic circuit corresponding to the two-element Windkessel model, where the total compliance μ and total vascular resistance η are connected in parallel. This configuration demonstrates how arterial pressure $\zeta(\tau)$ and blood flow $Q(\tau)$ are interrelated during the cardiac cycle, forming the mathematical foundation of the model described by (1.1).

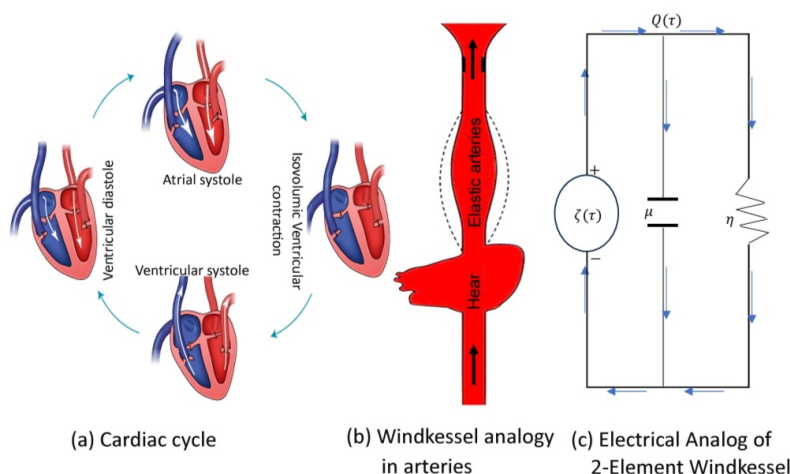


Figure 1. The 2-Element Windkessel model in human circulatory system.

In two-element Windkessel model, we have $Q(\tau) = \frac{v}{\tau}$ where v is the volume of blood being pumped at the time τ . Here we give some approximate solution of homogeneous part of Eq (1.2) by using the technique of ARPSM. Consider the following fractional differential equation in the usual topological Banach space $\mathcal{B} = \mathbb{R}$

$$\begin{cases} \mu {}^c\mathcal{D}^\delta \zeta(\tau) + \frac{1}{\eta} \zeta(\tau) = 0, & 0 < \delta \leq 1 \\ \zeta(0) = \mu, \end{cases} \quad (4.1)$$

where $\zeta(\tau)$ is the arterial pressure, η is the total vascular resistance and μ is the total compliance of the arterial system. It is clear that the exact solution of Eq (4.1) with the initial condition $\zeta(0) = \mu$ is $\zeta(\tau) = e^{-\frac{\tau}{\mu R}}$. Now we will use the technique of ARPSM to get approximate solution of (4.1) with the initial condition $r_0 = \mu$. Use Aboodh transforms on Eq (4.1) to get the following equation:

$$\zeta^A(\theta) = \frac{\mu}{\theta^2} + \frac{1}{\eta\mu\theta^\delta} \zeta^A(\theta) \quad (4.2)$$

with $\langle \zeta_n^A \rangle_{n \in \mathbb{N} \cup \{0\}}$

$$\zeta_n^A(\theta) = \frac{\mu}{\theta^2} + \sum_{j=1}^n \frac{r_j}{\theta^{j\delta+2}}. \quad (4.3)$$

The n -th terms of Eq (4.2)

$$\zeta_n^A(\theta) = \frac{\mu}{\theta^2} + \frac{1}{\eta\mu\theta^\delta} \zeta_n^A(\theta). \quad (4.4)$$

The Aboodh residual map, $A_\theta \mathcal{R}es \zeta$ for Eq (4.2) is given by

$$A_\theta \mathcal{R}es \zeta = \zeta^A(\theta) - \frac{\mu}{\theta^2} - \frac{1}{\eta\mu\theta^\delta} \zeta^A(\theta) \quad (4.5)$$

with the n -th Aboodh residual map

$$A_\theta \mathcal{R}es_n \zeta = \zeta_n^A(\theta) - \frac{\mu}{\theta^2} - \frac{1}{\eta\mu\theta^\delta} \zeta_n^A(\theta). \quad (4.6)$$

Now we calculate $\langle r_n \rangle_{n \in \mathbb{N} \cup \{0\}}$ by using the following relation

$$\lim_{\theta \rightarrow \infty} \theta^{n\delta+2} A_\theta \mathcal{R}es_n \omega = 0 \quad n = 1, 2, 3, \dots \quad (4.7)$$

At $n = 1$, by using Eq (4.3) we get that

$$\zeta_1^A(\theta) = \frac{\mu}{\theta^2} + \frac{r_1}{\theta^{\delta+2}}$$

and Eq (4.6) becomes

$$A_\theta \mathcal{R}es_1 \zeta^A(\theta) = \frac{r_1}{\theta^{\delta+2}} - \frac{1}{\eta\theta^{\delta+2}} - \frac{r_1}{\eta\mu\theta^{2\delta+2}}. \quad (4.8)$$

By multiplying both sides of Eq (4.8) by $\theta^{\delta+2}$ and by using Eq (4.7) we get $r_1 = \frac{1}{\eta}$. At $n = 2$, by using Eq (4.3) we get that

$$\zeta_2^A(\theta) = \frac{\mu}{\theta^2} + \frac{1}{\eta\theta^{\delta+2}} + \frac{r_2}{\theta^{2\delta+2}}$$

and Eq (4.6) becomes

$$A_{\theta} \text{Res}_2 \zeta^A(\theta) = \frac{r_2}{\theta^{2\delta+2}} - \frac{1}{\eta^2 \mu \theta^{2\delta+2}} - \frac{r_2}{\eta \mu \theta^{3\delta+2}}. \quad (4.9)$$

By multiplying both sides of Eq (4.9) by $\theta^{2\delta+2}$ and by using Eq (4.7) we get $r_2 = \frac{1}{\eta^2 \mu}$. At $n = 3$, by using Eq (4.3) we get that

$$\zeta_3^A(\theta) = \frac{\mu}{\theta^2} + \frac{1}{\eta \theta^{\delta+2}} + \frac{1}{\eta^2 \mu \theta^{2\delta+2}} + \frac{r_3}{\theta^{3\delta+2}}$$

and Eq (4.6) becomes

$$A_{\theta} \text{Res}_3 \zeta^A(\theta) = \frac{r_3}{\theta^{3\delta+2}} - \frac{1}{\eta^3 \mu^2 \theta^{3\delta+2}} - \frac{r_2}{\eta \mu \theta^{4\delta+2}}. \quad (4.10)$$

By multiplying both sides of Eq (4.10) by $\theta^{3\delta+2}$ and by using Eq (4.7) we get $r_2 = \frac{1}{\eta^3 \mu^2}$. Hence we get that

$$r_n = \frac{1}{\eta^n \mu^{n-1}} \quad \text{for all } n \in \mathbb{N} \cup \{0\}.$$

Then we put the values of $\langle r_n \rangle_{n \in \mathbb{N} \cup \{0\}}$ in Eq (3.6) to get

$$\zeta^A(\theta) = \sum_{j=0}^{\infty} \frac{1}{\eta^j \mu^{j-1} \theta^{j\delta+2}}. \quad (4.11)$$

By using the inverse Aboodh transform of Eq (4.11), we get

$$\zeta(\tau) = \sum_{j=0}^{\infty} \frac{\tau^{j\delta}}{\eta^j \mu^{j-1} \Gamma(j\delta + 1)}. \quad (4.12)$$

5. Numerical discussion

Table 1 uses ARPSM to present some approximate solutions of Caputo fractional Windkessel model (4.1) for several order values δ and via numerical imitation, the Figures 2–5 present the dynamical behaviour of solutions of Caputo fractional Windkessel model (4.1). Table 1 summarizes the numerical results obtained for the Caputo fractional Windkessel model using the ARPSM for fractional orders $\delta = 0.25$ and $\delta = 0.5$ at several values of μ , η , and τ . It provides computed values of the arterial pressure $\zeta(\tau)$ under different compliance and resistance conditions. The table clearly indicates that increasing μ (compliance) or η (resistance) slightly modifies the pressure amplitude, while the fractional order δ influences the rate of pressure decay. The close agreement between the results for $\delta = 0.25$ and $\delta = 0.5$ demonstrates the stability and reliability of the ARPSM. This numerical evidence supports the graphical observations in Figures 2–5 and confirms the method's high accuracy and convergence efficiency. Figure 2 displays the graphical behavior of the approximate solutions of the Caputo fractional Windkessel model obtained using the ARPSM when $\mu = 20$, $\eta = 22$, and fractional orders $\delta = 0.25$ and $\delta = 0.5$. The figure presents 3-D surface plots that demonstrate the evolution of arterial pressure $\zeta(\tau)$ with respect to time τ and the fractional order δ . The plots show that as δ increases, the system exhibits smoother decay and reduced oscillations, confirming the stabilizing effect of higher fractional orders. This behavior highlights the sensitivity of arterial pressure to fractional variations

and validates the flexibility of the ARPSM in describing fractional dynamics. Figure 3 shows the approximate solutions for the same fractional orders $\delta = 0.25$ and $\delta = 0.5$, but with a higher compliance value $\mu = 40$ and constant resistance $\eta = 22$. The results confirm that increasing the compliance leads to slightly higher steady-state arterial pressures and smoother transient behavior. The graphs further indicate that the ARPSM accurately reproduces the pressure-time relationship and maintains numerical stability for both fractional orders, demonstrating the method's robustness for physiological parameter variations. In Figure 4, the approximate solutions are obtained for $\mu = 60$, $\eta = 22$, and fractional orders $\delta = 0.25$ and $\delta = 0.5$. The surface plots reveal that as compliance μ increases, arterial pressure $\zeta(\tau)$ approaches a more constant profile, reflecting a slower decay rate. This agrees with physiological expectations that greater arterial compliance yields smoother and less oscillatory pressure responses. The fractional parameter δ continues to influence the relaxation rate of the pressure waveform, demonstrating the interplay between fractional dynamics and vascular elasticity. Figure 5 presents the results for $\mu = 80$, $\eta = 22$, and the same fractional orders $\delta = 0.25$ and $\delta = 0.5$. The graphs confirm that larger compliance values result in a nearly steady-state arterial pressure for all examined time intervals. The results visually support the convergence and stability of the ARPSM for larger physiological parameters. The method maintains consistent accuracy and convergence trends across different fractional orders, emphasizing its efficiency in capturing realistic circulatory dynamics. The results depicted in the preceding figures and tables clearly demonstrate the precision and efficiency of the ARPSM approach. The comparative tables highlight how the proposed scheme performs against several well-known techniques across different fractional-order parameters, while the corresponding graphical representations reveal consistent and symmetric trends among the three fractional derivatives. Furthermore, the obtained results confirm that ARPSM provides highly accurate approximations, closely matching both analytical and numerical benchmarks. The method's structured yet simple formulation eliminates the need for linearization, discretization, or perturbation procedures, thereby facilitating practical implementation. In addition, ARPSM generates rapidly convergent series solutions, ensuring numerical stability together with excellent precision. Another notable advantage of the method is its flexibility and applicability to a broad class of fractional differential equations—both linear and nonlinear of diverse fractional orders. From a computational viewpoint, ARPSM is computationally economical, achieving comparable accuracy to traditional numerical techniques with significantly fewer iterative steps. Its inherent inclusion of fractional integral and derivative operators makes it naturally compatible with modern fractional models. Finally, because the solutions are expressed as controllable power-series expansions, the accuracy can be easily tuned by adding further terms, enabling a practical trade-off between computational cost and precision.

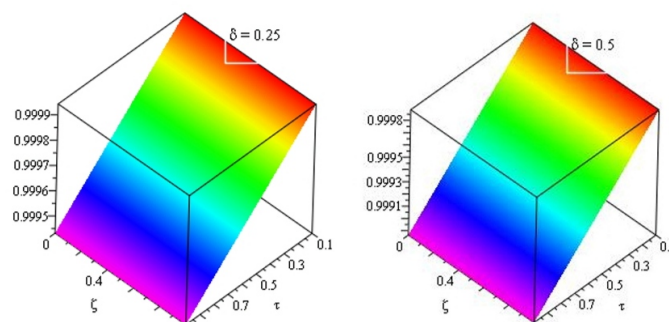


Figure 2. Some graphical solutions for (4.1) by using ARPSM with $\delta = 0.25, 0.5$, $\mu = 20$, $\eta = 22$ and some values of τ .

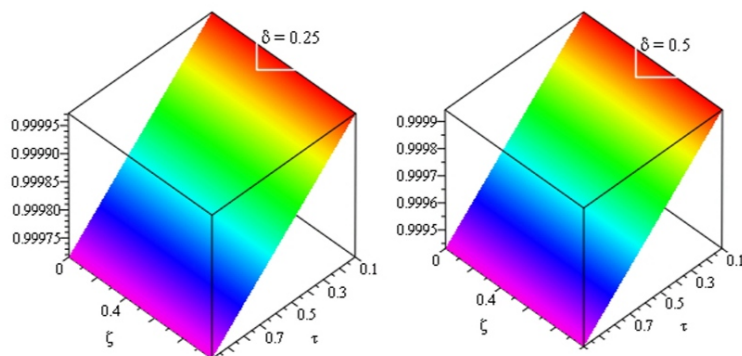


Figure 3. Some graphical solutions for (4.1) by using ARPSM with $\delta = 0.25, 0.5$, $\mu = 40$, $\eta = 22$ and some values of τ .

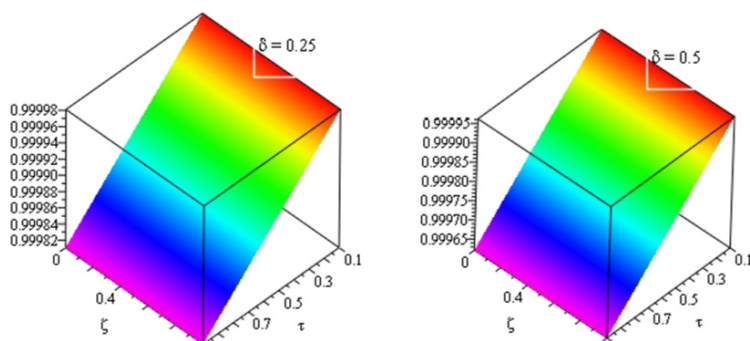


Figure 4. Some graphical solutions for (4.1) by using ARPSM with $\delta = 0.25, 0.5$, $\mu = 60$, $\eta = 22$ and some values of τ .

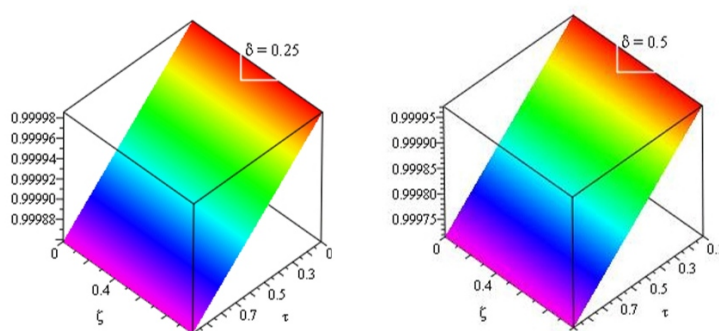


Figure 5. Some graphical solutions for (4.1) by using ARPSM with $\delta = 0.25, 0.5$, $\mu = 80$, $\eta = 22$ and some values of τ .

Table 1. Some numerical solutions of (4.1) by using ARPSM at $\delta = 0.25$ and $\delta = 0.5$ with several values of μ , η and τ .

			$\delta = 0.25$		$\delta = 0.50$			$\delta = 0.25$		$\delta = 0.50$	
μ	η	τ	$\zeta(\tau)$	$\zeta(\tau)$	η	μ	τ	$\zeta(\tau)$	$\zeta(\tau)$		
20	22	0.1	0.99994	0.99989	60	22	0.1	0.99998	0.99996		
		0.2	0.99989	0.99977			0.2	0.99996	0.99992		
		0.3	0.99820	0.99967			0.3	0.99994	0.99988		
		0.4	0.99977	0.99955			0.4	0.99992	0.99984		
		0.5	0.99971	0.99943			0.5	0.99990	0.99981		
		0.6	0.99965	0.99932			0.6	0.99988	0.99972		
		0.7	0.99960	0.99920			0.7	0.99986	0.99970		
		0.8	0.99954	0.99909			0.8	0.99984	0.99969		
		0.9	0.99948	0.99878			0.9	0.99982	0.99965		
		1.0	0.99943	0.99870			1.0	0.99981	0.99962		
40	22	0.1	0.99997	0.99994	80	22	0.1	0.99998	0.99997		
		0.2	0.99994	0.99988			0.2	0.99997	0.99994		
		0.3	0.99991	0.99982			0.3	0.99995	0.99991		
		0.4	0.99988	0.99977			0.4	0.99994	0.99988		
		0.5	0.99985	0.99971			0.5	0.99992	0.99985		
		0.6	0.99982	0.99965			0.6	0.99991	0.99982		
		0.7	0.99980	0.99960			0.7	0.99990	0.99980		
		0.8	0.99977	0.99954			0.8	0.99971	0.99977		
		0.9	0.99974	0.99948			0.9	0.99965	0.99974		
		1.0	0.99971	0.99943			1.0	0.99960	0.99971		

6. Conclusions

In this work, a new analytical framework has been developed to study the Caputo fractional Windkessel model representing the cardiovascular circulatory system within the structure of usual

topological Banach spaces. By employing the ARPSM, which integrates the Aboodh transform with the residual power series approach, approximate analytical solutions were successfully derived for the fractional differential form of the Windkessel model. The proposed method proved to be an efficient and systematic tool for handling fractional models due to its simple implementation, fast convergence, and high computational accuracy. The obtained results demonstrate that the ARPSM provides stable and reliable approximations that are consistent with the physiological interpretation of arterial pressure and blood flow behavior. Numerical and graphical analyses confirmed the method's capability to capture the influence of fractional parameters on circulatory dynamics, revealing that fractional orders offer a more realistic description of memory effects and viscoelastic properties in vascular systems. The combination of the Caputo derivative and Aboodh transform within Banach space topology not only broadens the theoretical foundation of fractional calculus but also enhances its applicability in biomedical and physical modeling. Overall, the findings of this study verify the robustness, reliability, and flexibility of the ARPSM in solving complex fractional differential equations. Future research may extend this approach to more intricate cardiovascular models or other biological and engineering systems governed by fractional dynamics, particularly those involving multi-dimensional, nonlinear, or time-dependent boundary conditions.

Use of Generative-AI tools declaration

The author declare that no AI tools were used in this work.

Conflict of interest

The author declares no conflicts of interest.

Acknowledgement

This work was supported and funded by the Deanship of Scientific Research at Taiz University.

References

1. Y. Jawarneh, H. Yasmin, M. M. Al-Sawalha, A. Khan, Fractional comparative analysis of Camassa–Holm and Degasperis–Procesi equations, *AIMS Math.*, **8** (2023), 25845–25862. <https://doi.org/10.3934/math.20231343>
2. B. Zhu, B. Hu, Approximate controllability for mixed-type non-autonomous fractional differential equations, *Qual. Theory Dyn. Syst.*, **21** (2022), 111. <https://doi.org/10.1007/s12346-022-00617-2>
3. B. Zhu, B. Hu, W. G. Yang, Existence of mild solutions for a class of fractional non-autonomous evolution equations with delay, *Acta Math. Appl. Sin. Engl. Ser.*, **36** (2020), 870–878. <https://doi.org/10.1007/s10255-020-0966-8>
4. F. H. Damag, A. Saif, On solving modified time Caputo fractional Kawahara equations using Laplace residual power series method, *Fractal Fract.*, **9** (2025), 301. <https://doi.org/10.3390/fractalfract9050301>

5. K. Shah, A. R. Seadawy, M. Arfan, Evaluation of one-dimensional fuzzy fractional partial differential equations, *Alex. Eng. J.*, **59** (2020), 3347–3353. <https://doi.org/10.1016/j.aej.2020.05.020>
6. S. Kılıç, E. Çelik, Complex solutions to the higher-order nonlinear Boussinesq-type wave equation transform, *Ric. Mat.*, (2022). <https://doi.org/10.1007/s11587-022-00698-1>
7. B. Zhu, L. Li, Y. Wu, Local and global existence of mild solutions for nonlinear fractional reaction–diffusion equations with delay, *Appl. Math. Lett.*, **61** (2016), 73–79. <https://doi.org/10.1016/j.aml.2016.05.007>
8. F. H. Damag, On comparing analytical and numerical solutions of time Caputo fractional Kawahara equations, *Mathematics*, **13** (2025), 2995. <https://doi.org/10.3390/math13182995>
9. B. Hu, B. Zhu, Existence and stability of mixed-type Hilfer fractional differential equations with impulses and time delay, *Results Appl. Math.*, **28** (2025), 100653. <https://doi.org/10.1016/j.rinam.2024.100653>
10. A. Akgül, A. Cordero, J. R. Torregrosa, A fractional Newton method with 2α -order of convergence and its stability, *Appl. Math. Lett.*, **98** (2019), 344–351. <https://doi.org/10.1016/j.aml.2019.06.017>
11. F. H. Damag, A. Saif, A. Kılıçman, ϕ -Hilfer fractional Cauchy problems with almost sectorial and Lie bracket operators, *Fractal Fract.*, **8** (2024), 741. <https://doi.org/10.3390/fractalfract8120741>
12. T. Yazgan, E. İlhan, E. Çelik, H. Bulut, New hyperbolic wave solutions to Wu–Zhang system models, *Opt. Quantum Electron.*, **54** (2022), 298. <https://doi.org/10.1007/s11082-022-03726-4>
13. D. Burkhoff, J. Alexander, J. Schipke, Assessment of Windkessel as a model of aortic input impedance, *Am. J. Physiol. Heart Circ. Physiol.*, **255** (1988), H742–H753. <https://doi.org/10.1152/ajpheart.1988.255.4.H742>
14. F. Duronio, A. Di Mascio, Blood flow simulation of aneurysmatic thoracic aorta using OpenFOAM, *Fluids*, **8** (2023), 272. <https://doi.org/10.3390/fluids8100272>
15. G. Gnudi, Analytical solution to Windkessel models using piecewise linear aortic flow waveform, *Physiol. Meas.*, **44** (2023), 06NT01. <https://doi.org/10.1088/1361-6579/acd6cd>
16. A. Gil, R. Navarro, P. Quintero, A. Mares, Transient performance analysis of left ventricular assist devices coupled with Windkessel model, *J. Biomech. Eng.*, **146** (2024). <https://doi.org/10.1115/1.4064974>
17. M. Fernandes, L. C. Sousa, C. A. António, S. I. Pinto, Modeling the five-element Windkessel using blood viscoelasticity, *Mathematics*, **11** (2023), 4877. <https://doi.org/10.3390/math11244877>
18. N. Westerhof, J. W. Lankhaar, B. E. Westerhof, The arterial Windkessel, *Med. Biol. Eng. Comput.*, **47** (2009), 131–141. <https://doi.org/10.1007/s11517-008-0359-2>
19. A. D. Choudhury, R. Banerjee, A. Sinha, S. Kundu, Estimating blood pressure using Windkessel model on PPG, *Proc. IEEE Eng. Med. Biol. Soc.*, (2014), 4567–4570. <https://doi.org/10.1109/EMBC.2014.6944642>
20. T. Kind, T. J. Faes, J. W. Lankhaar, A. Vonk-Noordegraaf, M. Verhaegen, Estimation of three- and four-element Windkessel parameters, *IEEE Trans. Biomed. Eng.*, **57** (2010), 1531–1538. <https://doi.org/10.1109/TBME.2010.2046487>

21. T. Gamilov, Y. Ruslan, Fractional-order Windkessel boundary conditions, *Fractal Fract.*, **7** (2023), 373. <https://doi.org/10.3390/fractalfract7050373>
22. A. Bahloul, T. Taous, Assessment of fractional-order arterial Windkessel, *IEEE Open J. Eng. Med. Biol.*, **1** (2020), 123–132. <https://doi.org/10.1109/OJEMB.2020.2990498>
23. J. E. Traver, C. Nuevo-Gallardo¹, I. Tejado¹, J. Fernández-Portales, J. F. Ortega-Morán, J. Blas Pagador, et al., Cardiovascular circulatory system and left carotid model: A fractional approach, *Fractal Fract.*, **6** (2022), 64. <https://doi.org/10.3390/fractalfract6020064>
24. V. L. Resmi, N. Selvaganesan, Fractional-order arterial Windkessel model via optimization, *IETE J. Educ.*, **64** (2023), 103–111. <https://doi.org/10.1080/09747338.2021.2016751>
25. B. E. Belinskii, R. T. Liflyand, The Banach algebra A and its properties, *J. Fourier Anal. Appl.*, **3** (1997), 103–129. <https://doi.org/10.1007/BF02649131>
26. F. H. Damag, A. Kılıçman, A. T. Al-Arioi, On hybrid-type nonlinear fractional integro-differential equations, *Mathematics*, **8** (2020), 984. <https://doi.org/10.3390/math8060984>
27. M. A. Oqielat, T. Eriqat, O. Ogilat, A. El-Ajou, S. E. Alhazmi, S. Al-Omar¹, Laplace residual power series method for solving time-fractional reaction–diffusion model, *Fractal Fract.*, **7** (2023), 309. <https://doi.org/10.3390/fractalfract7040309>
28. S. Noor, W. Albalawi, R. Shah, M. M. Al-Sawalha, S. M. E. Ismaeel, S. A. El-Tantawy, Approximations to fractional nonlinear damped Burgers-type equations, *Front. Phys.*, **12** (2024), 1374481. <https://doi.org/10.3389/fphy.2024.1374481>
29. M. I. Liaqat, A. Akgül, H. Abu-Zinadah, Time-fractional Black–Scholes models via Aboodh residual power series, *Mathematics*, **11** (2023), 276. <https://doi.org/10.3390/math11020276>
30. H. Yasmin, A. H. Almuqrin, Analytical study of time-fractional heat, diffusion and Burgers equations, *AIMS Math.*, **9** (2024), 16721–16752. <https://doi.org/10.3934/math.2024837>
31. S. A. Edalatpanah, E. Abdolmaleki, Aboodh residual power series for fractional Newell–Whitehead–Segel equation, *Comput. Algorithms Numer. Dimens.*, **3** (2024), 115–131. <https://doi.org/10.1007/s44243-024-00052-0>
32. M. Catanho, M. Sinha, V. Vijayan, Model of aortic blood flow using the Windkessel effect, *Univ. California San Diego, Tech. Rep.*, (2012).



AIMS Press

©2025 the Author(s), licensee AIMS Press. This is an open access article distributed under the terms of the Creative Commons Attribution License (<https://creativecommons.org/licenses/by/4.0>)